# The hydrophobic force: measurements and methods

**Rico F. Tabor,*[a] Franz Grieser,[b,c] Raymond R. Dagastine[b,d,e] and Derek Y. C. Chan[b,f,g]**

***Received Xth XXXXXXXXXX 20XX, Accepted Xth XXXXXXXXX 20XX***

***First published on the web Xth XXXXXXXXXX 200X***

**DOI: 10.1039/b000000x**

The hydrophobic force describes the attraction between water-hating molecules (and surfaces) that draws them together, causing aggregation, phase separation, protein folding and many other inherent physical phenomena. Attempts have been made to isolate the range and magnitude of this interaction between extended surfaces for more than four decades, with wildly varying results. In this perspective, we critically analyse the application of common force-measuring techniques to the hydrophobic force conundrum. In doing so, we highlight possible interferences to these measurements and provide physical rationalisation where possible. By analysing the most recent measurements, new approaches to establishing the form of this force become apparent, and we suggest potential future directions to further refine our understanding of this vital, physical force.

## The hydrophobic force

The hydrophobic force underlies many common processes: the separation of oil and water, the beading up of water droplets on the leaves of waxy plants, and the aggregation and folding of certain molecules into micelles, liquid crystals, cell membranes, enzymes, *etc*. It can therefore be seen that this force is central to the mechanisms at the core of life, both biological and chemical.[1] Of course this force must be considered within the framework of existing surface and structural interactions that drive processes and stability, including electrostatics, van der Waals, steric and solvation forces. The physical driving force that underlies hydrophobic phenomena is simply that water specifically orients near non-polar surfaces, adversely affecting its 3D hydrogen bonding network and losing configurational entropy.[2] By minimising the contact between non-polar surfaces and water molecules, water configurational entropy increases. Therefore, when two such non-polar objects are brought into sufficiently close proximity (Fig. 1), the hydrophobic effect is experienced as an attractive force between them – the hydrophobic force.

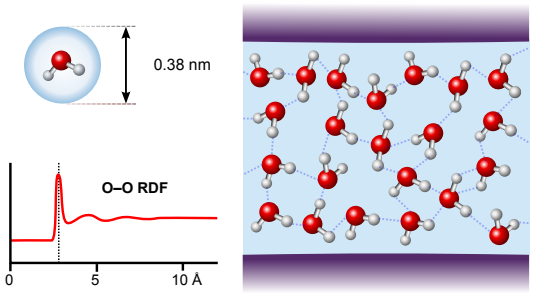


**Fig. 1** Structural and dimensional considerations for liquid water: from volume and density considerations, the average volume per water molecule in liquid water is $\approx 3 \times 10^{-24}$ m$^3$; if treated as a sphere, this gives a diameter of 3.8 Å. Radial distribution function data from neutron diffraction measurements of liquid water[3] indicate an average O–O separation of ≈2.8 Å.

The hydrophobic force is perhaps best interpreted as a specific meso- or macro-scopic manifestation of the hydrophobic effect[4] – that is, the antipathy of water for non-polar surfaces or molecules. For these reasons, the various terms 'hydrophobic attraction' and 'hydrophobic interaction' have arisen in the literature; here, we use 'hydrophobic force' throughout. The level of hydrophobicity of a solid surface is generally defined by its contact angle with water in air, wherein values above 90°(measured through the water) are considered hydrophobic. Similarly for water–liquid interfaces (*e.g.* water–oil), interfacial tension is an indicator of the liquid's hydrophobicity, with larger values pointing to greater hydrophobicity. As the posited origin of the hydrophobic force is entropic, it would be expected that a strong temperature dependence would be seen. This is indeed realised in both experimental[5] and

[a] *School of Chemistry, Monash University, Clayton, VIC 3800, Australia. Fax: +61 3 9905 4597; Tel: +61 3 9905 4558; E-mail: rico.tabor@monash.edu*

[b] *Particulate Fluids Processing Centre, The University of Melbourne, Parkville 3010, Australia.*

[c] *School of Chemistry, The University of Melbourne, Parkville 3010, Australia.*

[d] *Department of Chemical and Biomolecular Engineering, The University of Melbourne, Parkville 3010, Australia.*

[e] *Melbourne Centre for Nanofabrication, 151 Wellington Road, Clayton, Victoria, 3168, Australia*

[f] *Department of Mathematics and Statistics, The University of Melbourne, Parkville 3010, Australia.*

[f] *Department of Chemistry and Biotechnology, Swinburne University of Technology, Hawthorn 3122, Australia*

modelling[6] studies on this topic.

A number of excellent reviews cover the mechanistic rationale of, and attempts to measure, the hydrophobic force, along with progress from theoretical modelling; these are only summarised briefly here. The interested reader is directed to more extensive references for experimental progress[7–10] and for details of theoretical modelling[11].

The purpose of this article is to critically analyse the methodology used in direct measurements of the hydrophobic force between extended and mesoscopic surfaces to date, to highlight possible interferences to these measurements, and to indicate improvements that can be made and future avenues of research to further our understanding of the hydrophobic force.

Since Tanford's pioneering work on the role of the hydrophobic effect in the aggregation of molecules,[1,12–14] considerable effort has been applied to direct measurements of the interaction force between hydrophobic objects in water. The rationale underlying these measurements is that if it is possible to directly quantify the force between such objects, a greater understanding of biological and chemical pathways and mechanisms will be obtained, as well as providing an opportunity to design devices and processes that exploit and control the hydrophobic force. An obvious issue however is that the force measurement techniques available work with extended (macroscopic) surfaces – this disparity in length scales becomes an overriding concern when attempting to measure a force mediated by water molecules that are only a fraction of a nanometre in size (Fig. 1).

In order to contextualise the often paradoxical length-scales seen in literature reports of hydrophobic forces, it is pertinent to consider the size and structure of water molecules in the liquid phase. Bulk measurements using neutron diffraction and modelling have indicated that on average, the oxygen atoms of neighboruring water molecules are $\approx$2.8 Å apart in the liquid phase at standard temperature and pressure.[3] Specular X-ray reflectivity suggests this distance decreases slightly to 2.5-2.7 Å for water molecules adjacent to mica surfaces.[15] Strong evidence for 'layering' of water molecules adjacent to solid surfaces has been seen using frequency-modulated atomic force microscopy (FM-AFM).[16–19] In all of these cases, characteristic intermolecular spacings of $3 \pm 0.5$ Å are noted.

There are a number of recently observed phenomena that provide additional context to the role of water structure, particularly when considering dynamic measurements. Two of the most important considerations are the viscosity of water that is confined within nanometre-sized layers (so-called nanoconfinement), and the potential for boundary condition changes due to the interaction of the water and the hydrophobic surfaces. It seems likely that both of these effects are linked to the unique hydrogen bonding structure of water near surfaces, and thus are certainly pertinent to a discussion of the hydrophobic force. It has been shown both theoretically and experimentally that water in highly confined geometries – a few nanometres or less – changes its properties. The viscosity is seen to increase by varying amounts depending on the level of confinement,[20,21] which is perhaps unsurprising for a highly hydrogen bonded liquid under molecular-level confinement. Ortiz-Young *et al.* noted significant dependence of interfacial viscous forces on substrate wettability,[21] with hydrophobic surfaces experiencing the lowest force due to apparent interfacial slip; they concluded that the intrinsic viscosity of water was however substrate independent. Connected to dynamic viscosity increases, the orientation relaxation of water molecules in confined geometries may be arrested significantly,[22] again pointing to strong interactions due to hydrogen bonding.

The subject of water slip at solid surfaces – whereby the boundary condition is such that water directly in contact with the solid surface has a non-zero velocity when the bulk liquid undergoes flow – has proven controversial, although both experiments and theoretical studies have demonstrated the effect.[23,24] In fact, recent modelling has shown that even hydrophilic surfaces may result in boundary slippage of water.[25]

As our ability to measure such transient and molecular level effects increases, we must be prepared to account for their effects within our measurements and interpretation of the hydrophobic force.

## Force measurement techniques and their application to study of the hydrophobic force

As noted by Christenson and Claesson,[7] the measurement of surface forces between objects in water is a relatively new topic of investigation, with the most significant advances having been made in the last four decades, after pioneering work by Derjaguin and others.[26] Such force measurements fall into two broad classes: 1) those in which liquid is extracted from the film between two deformable surfaces (usually air-water interfaces) or one deformable and one solid surface, and the pressure of the liquid in the film is measured - examples include the Thin-Film Balance (TFB) and the closely-related Scheludko-Exerowa cell;[27] and 2) those in which one object is brought towards another and the

force (and if possible, the separation) is measured - this class includes the Surface Forces Apparatus (SFA) and the Atomic Force Microscope (AFM). These measurement techniques are shown schematically in Figure 2, along with the typical form of the data obtained.

Here we focus only on force measuring techniques that have been applied to the specific study of hydrophobic interactions. Other force measurement apparatus have been devised that will not be discussed, but the interested reader is directed to reviews on the topic.[28,29] At larger length-scales, measurement of surface forces has recently been achieved using the Integrated Thin Film Drainage Apparatus (ITFDA),[30] with the potential to access dynamic forces at much larger Reynolds number than can be achieved with the AFM. Also of interest is Total Internal Reflection Microscopy (TIRM),[31] a method of measuring the energy profile between a levitated particle or droplet and a surface, with phenomenal precision down to the equivalent of femtoNewton levels. Although this has not yet been applied to study of the hydrophobic force due to the unique demands of such an experiment, the development of such techniques may improve resolution of hydrophobic force measurements in the future.

Perhaps the first concerted attempt to measure a hydrophobic effect via a force balance was in the work of Blake and Kitchener,[32] observing liquid films between a gas bubble and hydrophilic or hydrophobic silica in water using interferometry. They noted that aqueous films on the hydrophobic (methylated) surfaces tended to rupture at a critical thickness, and apportioned this to *"reduced hydrogen bonding at the solid–water interface"*. Although this measurement method could not directly quantify the interaction, the interpretation and mechanism as posited has not changed greatly in the intervening 40+ years. What has advanced is our ability to measure the range and magnitude of the force, and thus deduce its functional form.

Although such film balance measurements using deformable interfaces can theoretically determine the disjoining pressure – that is, the pressure in the liquid film due to surface forces such as double-layer, van der Waals and hydrophobic interactions – as a function of film thickness, in practice a number of constraints make this a difficult task. The most significant is that the van der Waals force is large and attractive for air-water-air systems[33] (Hamaker constant, $A_{awa} \approx 4 \times 10^{-20}$ J) resulting in film rupture at large thicknesses, thus missing any short-ranged (sub-nanometre) attractive effects. Some reports using film balance measurements have suggested longer range 'hydrophobic' effects for surfactant-stabilised systems,[34] although quantification and unambiguous interpretation here is challenging. Furthermore, molecular dynamics simulations

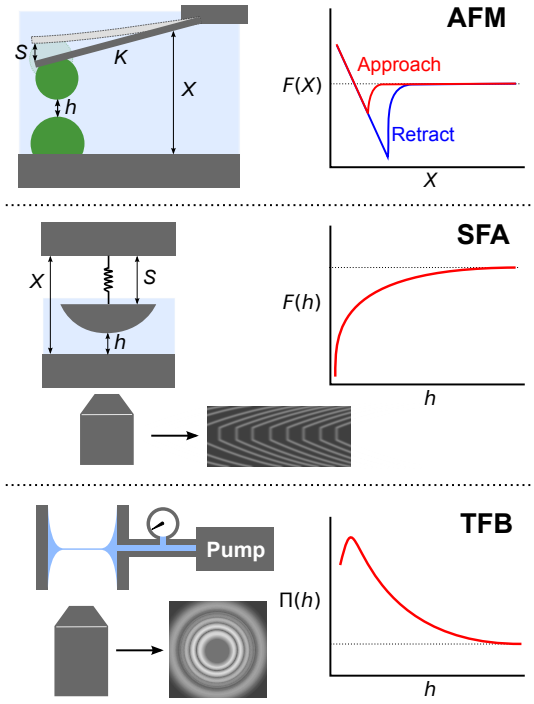


**Fig. 2** The three most common force measurement methods that have been historically used to obtain information on the range and strength of the hydrophobic force. On the left is shown a schematic of the instrument itself, and on the right is schematically shown the typical form of the data obtained.

of liquid films in the thin film balance geometry without surfactant indicate that the calculated Hamaker function underpredicts the attractive force in these films,[35] as Lifshitz theory as applied does not account for fluid density changes or solution structuring within the film. This suggests a possible alternative reason for the observation of a long range attraction other than a hydrophobic force.

To result in a 'true' force *vs* separation curve, the distance between approaching interfaces, *i.e.*, the thickness of the water film in measurements of the hydrophobic force, must be obtained, and this is generally achieved by interferometric measurement for the TFB and SFA. This is usually calibrated by counting backwards from the point of contact or film rupture, and for the SFA, the level of resolution achieved is sub-nanometre.[36] The resolution of film thickness obtained by the TFB depends on the optical parameters of the system, but is typically limited to a few nanometres, and for very thin films, quantification is challenging. In the AFM, the thickness of the intervening liquid film can be obtained by calibration from surface contact for rigid systems with nanometre precision, or by theoretical mod-

elling[37] or confocal microscopy[38] for deformable surfaces, although resolution is currently limited to tens of nanometres for the latter. In force measurements relying on springs of known force constant, including SFA and AFM, it is pertinent to note that force measurements must be made as surfaces are *approaching* one another, as adhesion may occur at contact, masking any short-range forces on retraction.

A selection of posited hydrophobic force laws from experimental measurements are plotted in Figure 3 for comparative purposes. It can be seen that these vary widely in both magnitude and length-scale, indicating that different physical systems and measurement methods result in quite different apparent force behaviour.

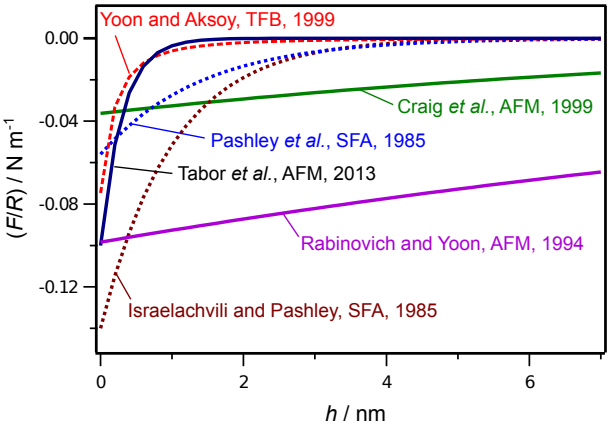


**Fig. 3** Hydrophobic force laws derived from experimental measurements using the AFM (solid lines), SFA (dotted lines) and TFB (dashed line). Data are redrawn from Yoon and Aksoy,[34] Craig *et al.*,[39] Pashley *et al.*,[40] Tabor *et al.*,[41] Rabinovich and Yoon[42] and Israelachvili and Pashley.[43]

## Potential sources of interference

As noted above, each force measurement technique has inherent benefits and limitations, and thus is more or less prone to certain interferences or effects that may inhibit a pure appraisal of the hydrophobic force. Below we identify potential factors – shown schematically in Figure 4 – that may interfere with a 'pure' measurement of the hydrophobic force and explain their significance in the context of previous measurements.

### Bubbles and adsorbed gas

It has recently become clear that nanobubbles – wide, flat gas domains with lateral dimension of hundreds of nanometres, but heights of only tens of nanometres – can be found on a wide range of solids, from pure materials such as graphite to surfaces decorated with adsorbed or chemically grafted species such as surfactants or silanes.[44–46] On hydrophobic surfaces, they have been visualised and probed using AFM imaging[44], Small-Angle Xray Scattering (SAXS),[47] and Total Internal Reflection Fluorescence microscopy (TIRF),[48] and their existence is now accepted; some studies even find them on conventionally hydrophilic surfaces such as mica.[49] Recent work by Yang *et al.* demonstrates the effect of AFM imaging mode and parameters during experiments on the information obtained,[50] enforcing the necessity of low-force techniques for the accurate reconstruction of their topology.

The mechanistic reason for the remarkable stability (over hours to days) of such surface nanobubbles is still unclear; according to conventional continuum thermodynamics models of bubble behaviour they should dissolve within seconds. Attempting to solve this puzzle has formed the basis for a very active and intense research effort as evidenced by recent reviews,[46,51] with explanations ranging from contamination[52] to diffusive 'refuelling' of the bubbles with gas.[53] Recent work has implicated once again the role of experimentally-introduced contamination on the stability of nanobubbles,[54] indicating potential reasons for the huge variability in their size, distribution and properties as measured in different reports.

The clear identification of where bubbles come from *in general* in bulk liquids and at surfaces has never been satisfactorily dealt with in the force literature. The creation of a cavity in bulk water (homogeneous cavitation) requires applied forces that can overcome the tensile strength of the liquid. For pure water this means either temperatures around 300°C or pressure drops that are in excess of 1000 bar.[55,56] It is often assumed that the creation of a cavity at a surface (heterogeneous cavitation), be it hydrophobic or hydrophilic, is significantly less than this, but this is not correct. Heterogeneous cavitation would require similar conditions as homogeneous cavitation as the liquid molecule solid interaction is very similar in magnitude to liquid molecule-liquid molecule interactions. One likely source of bubbles on a surface in contact with water would be from pre-existing gas nuclei captured when water initially makes contact with the surface; probably in defects on the surface. Another, and more general source, is from thermal spikes constantly deposited by background radiation. Background radiation, *e.g.*, cosmic radiation, has been shown to generate cavities in a liquid and these sites are responsible for lowering the apparent tensile strength of the liquid.[57] Once these cavities are created they must be stabilised, and a surface defect is a likely location for this to occur. It is probably from these sites

that microbubbles evolve, as Apfel has explored in his study.[58]

Regardless, it can be seen in many literature reports of forces measured between hydrophobic surfaces that nanobubbles play a central role in the forces observed, causing capillary-type interactions between hydrophobised solid surfaces out to hundreds of nanometres, and obscuring any short-range forces that may be present. In fact, several studies have purposefully generated nanobubbles on hydrophobic surfaces to probe forces between nanobubble-decorated surfaces using colloidal probe AFM.[59,60] From a quantitative force measurement perspective, this is quite challenging as the number and position of the nanobubbles are unknown during the force measurement itself, only that they are present with a significant surface density as imaged by AFM in control measurements. Instead these studies correlate the general force behavior to adhesion forces, frictional forces,[61] solvent conditions and most notably contact angle of microscopic air bubbles on surfaces.[60,62] This presents interesting implications, as these studies do not necessarily seek to determine the underlying thermodynamic origins of an intrinsic hydrophobic force, but develop a more pragmatic knowledge of how nanobubbles or this 'extrinsic hydrophobic force' can impact on dispersion behavior such as long range attractive forces, bubble attachment to surfaces and even dispersion rheology.[60] Confusion sometimes may arise as the literature often does not differentiate intrinsic forces due to water structuring effects from extrinsic forces due to adsorbed gas or bubbles in these scenarios.

Several recent studies have used purposefully textured surfaces to explore the forces experienced by superhydrophobic surfaces,[61,63,64] with the incidental effect of trapping significant gas pockets at the solid-water interface. This provides further confirmation on the role of micro- to meso-scopic gas domains on the forces between hydrophobic solid surfaces, in the form of strong and long-ranged bridging interactions, seen as characteristics steps and strong adhesions in the measured force curves with lengthscales up to several hundred nanometres.

Ishida and others have demonstrated that degassing the water phase has a significant effect on the measured forces between hydrophobised surfaces,[67] emphasising the role of bubbles and dissolved gas. Clearly in 'real' systems with extended hydrophobic solid surfaces, these bubbles would be an overriding issue, obscuring any shorter range, molecular based hydrophobicity. Indeed, modelling studies have shown that solid surfaces are gas-philic in water,[68,69] and so it not surprising that gas and nanobubble accumulation occurs at their interface with water. The problem of bubbles is clearly limited to solid surfaces, as bubbles cannot be retained at air-water or oil-water interfaces; their ubiquity on solids suggests that caution should be exercised with all hydrophobised solid surfaces. Although it has been shown that bubbles can form lenses at some oil-water interfaces,[70] these tend to be macroscopic, as the high gas solubility in oil means that small bubbles dissolve extremely rapidly (over a few seconds). The most likely reason for this mismatch between solid and liquid surfaces of similar hydrophobicity is that the air-liquid contact line can be pinned at a solid–liquid interface but cannot at a liquid–liquid interface.

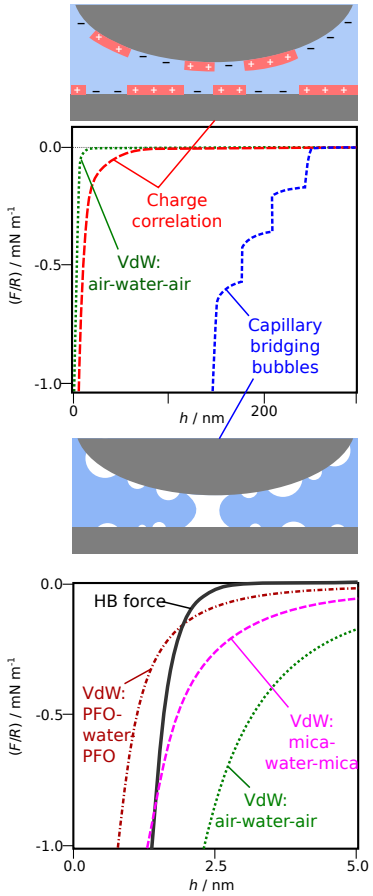


**Fig. 4** Typical interferences with measurements of the hydrophobic force. The lower panel compares the range and magnitude of typical van der Waals interactions with the most recently posited hydrophobic force law.[41] PFO = perfluorooctane. Data for charge correlation was redrawn from Meyer *et al.*[65] and for capillary bridging bubbles from Parker *et al.*[66]

In summary, although surface nanobubbles have been demonstrated by many groups to exist on solid surfaces, and certainly pose a fascinating thermodynamic enigma, their presence does not relate to the intrinsic hydrophobic force. Rather, their in-

fluence on force behaviour is more simply explained by continuum mechanical models of capillary bridges between surfaces, acting at much longer ranges than could be expected from water structuring. Thus it is appropriate to make a distinction here between the intrinsic hydrophobic force, arising from disruptions to the preferred orientation of water molecules alone, and extrinsic mechanisms that have origins of other types – further examples of which are discussed below. Of course, one could expect a hydrophobic force to act at the interface between two bubbles on approaching surfaces, as the bubbles themselves are intrinsically hydrophobic. However, such subtleties cannot be extracted from force measurements between surfaces decorated with the insufficiently well-defined nanobubbles described above.

**Solids and chemical hydrophobisation**

Another inherent problem with solid surfaces that are hydrophobised with molecular materials is that complex surface chemistry can come into play. For example, the effects of surface roughness are comparatively difficult to quantify in direct force measurements, as discussed below. Given the expected range of the hydrophobic force, even minimal roughness beyond the atomic level could overwhelm the ability to measure forces and separations accurately. Methods to overcome this problem include utilising surfaces that are inherently smooth due to a cleaved crystal plane (such as mica or highly-ordered pyrolytic graphite, HOPG) or making surfaces using techniques that retain exceptionally low roughness such as atomic layer deposition. Although HOPG is intrinsically hydrophobic, mica is not, and must therefore be hydrophobised chemically in order to present a surface suitable for measurement of the hydrophobic force.

As mica is the most commonly used substrate for SFA measurements, its chemical hydrophobisation has been an important concern. Original measurements used a cationic surfactant to form a monolayer on the mica surface.[43] However, additional complexity arises due to the ability of the molecules to move around on a highly dynamic (sub-millisecond) timescale, form bilayers and exist in dissociated and non-dissociated forms. It has been proposed that rearrangements can cause oppositely charged molecular 'patches' on the surfaces, resulting in a long-range charge attraction,[71,72] although a direct experimental link between such patches and measured forces has not yet been made. Similarly to the observation of the effects in force behaviour from nanobubbles, charge correlations clearly do not represent a hydrophobic force, with an explanation unconnected to the structuring of water or the hydrophobic characterstics of the materials employed.

Certainly an added complexity with surfactant monolayers is that at very small separations, the layers may fuse into a bilayer that bridges the two surfaces. The mechanics of this process was demonstrated elegantly in the SFA by use of a photo-isomerisable surfactant to exert subtle control over the surfactant layers,[73] providing direct insight into the strong, short-ranged forces experienced by surfaces undergoing bilayer hemifusion.

Other methods of chemical hydrophobisation include use of materials, such as octadecyltrichlorosilane (OTS), that react with the surface and are thus molecularly anchored.[74] Although this alleviates concerns about charge dissociation and molecular rearrangements, these surfaces may be somewhat rough (on the scale of a few nanometres),[74] making quantification at nanometre separations challenging.

If anything, the issues associated with both adsorbed gas and the variability in surface hydrophobisation techniques indicate that a thorough understanding of the physical and chemical constitution of the surface prior to force measurement is paramount. Indeed, AFM imaging is a valuable technique for assessing these features, particularly in the case of self-assembled surfaces such as lipid monolayers, whereby the act of perturbing the surface during imaging or force measurement may cause irreversible structural changes.[75]

Revealingly, literature reports have found differing outcomes when measuring the hydrophobic force for chemically hydrophobised surfaces possessing different water contact angles. Ishida *et al.* found a marked dependence of the measured force on contact angle for surfaces chemically hydrophobised with surfactants or OTS.[76] Hato however noticed a more complex dependence when dealing with mixed surfactant monolayers,[77] where differences between long- and short-range components of the measured forces were clear. Such differences point to a problem with reproducibility between measurement protocols, most likely resulting from differences in surface chemical hydrophobisation, and emphasising the importance of consistent and comparable methodologies.

It is clear from the differing outcomes of experiments that make use of chemical hydrophobisation that such methods are fraught with complexity and incidental issues that must be carefully considered in the analysis of such data.[78] This is further evidence that future techniques and measurements must find approaches that use surfaces that are intrinsically hydrophobic without adsorbed or bonded molecular agents, or must otherwise carefully account for the topology, surface chemistry and stability of such layers.

**Convolution with other forces**

In virtually all systems comprising extended surfaces, van der Waals and electrical double-layer interactions play an important role. For like materials interacting through water, the van der Waals force is attractive. The interaction arises from the correlations of quantum fluctuations in electrical dipole moments and is thus calculable from the dielectric functions of the materials using Lifshitz'a theory.[79] The limitation is that it can therefore only be known with the same precision to which the dielectric functions of the materials involved are known. Particularly for water-hydrocarbon/fluorocarbon systems that have similar absorption spectra in the UV, different constructions of the dielectric functions involved result in significant variations in the predicted forces,[33] inhibiting attempts to isolate the hydrophobic attraction with precision. The van der Waals force tends to be very large in magnitude at small separations ($< 10$ nm), but due to retardation effects from the finite speed of light, the interaction dies away rapidly at larger separations, as is seen for typical material combinations used for measuring the hydrophobic force in Figure 4. An added complication arises from using layered systems or surface coatings, such as adsorbed material on mica surfaces. At large separations, the van der Waals interaction is primarily due to the bulk material, but at very small separations the interaction becomes dominated by the Hamaker function of the surface layer.[80,81] This may make it more challenging to reliably model and subtract the van der Waals force for such systems.

Electrical double-layer interactions arise from the presence of bound or adsorbed ions or charged groups on the surface and their associated 'cloud' of counter-ions. When two surfaces thus decorated with uniform charge density are brought into proximity, the overlap of their diffuse layers results in a repulsion (or attraction if the surfaces are oppositely charged or have potentials of very different magnitudes). The surface charging behaviour of mica–water, air–water and oil water interfaces has been characterised for a range of solution conditions,[82,83] demonstrating that each experiences significant pH effects on the surface charge, and shows a well defined isoelectric point between pH 2 and 4. The effects of double layer interactions can be minimised by working at conditions in which the surfaces bear a net neutral charge, or by screening the force by the addition of electrolyte to reduce the effective Debye length.

An interesting aside that will not be covered in detail here is the so-called Hofmeister effect,[84] whereby different ions seem to exhibit systematic variations in their physicochemical behaviour,[85] which can cause significant changes in the stability and aggregation kinetics of colloidal systems.[86] The reason for this ion dependency is not entirely clear despite many studies attempting to elucidate the root cause, although it would appear to be connected to the fact that some solutes and ions tend to increase the local order in water (so-called kosmotropes) whereas others disrupt order (chaotropes). Our recent experiments measuring the hydrophobic force in concentrated salt conditions surprisingly found no differences when pairs of ions at either extreme of the Hofmeister series were used.[41] Theoretical work by Parsons *et al.* suggests that the electronic polarizability of different ions can modify the effective short-range van der Waals interaction between charged surfaces,[87] although this has yet to be verified experimentally.

To summarise, it can be seen that for most systems conventionally used to measure the hydrophobic force: air–water–air combinations in the thin film balance, mica–water–mica in the SFA or silica–water–silica in the AFM, any hydrophobic interaction is usually convolved with both double-layer and van der Waals forces. To obtain the pure hydrophobic force potential, these effects must be subtracted from the measured force. The precision with which this can be achieved is clearly dependent on the relative magnitude of the convolving forces and the accuracy with which they can be measured and modelled; for the expected very short range intrinsic hydrophobic force, this deconvolution represents a considerable problem.

Several recent approaches that may provide a new direction to the problem of convolved forces are discussed in the 'Recent advances' section below. Two appealing methods are a) to use extended interfaces that cannot sustain bubbles or experience classical forces,[41,88] and b) to use a working interface/probe that is sufficiently small so that exposure to these convolving forces is minimised.[21,89] The sharp tip of an AFM cantilever satisfies the requirements of the latter, whereas molecularly-smooth oil-water interfaces can be used for the former.

**Surface roughness**

Similarly to van der Waals forces, surface roughness is a property that pervades almost all 'real' systems. It is no coincidence that mica is such a widely used surface in force measurements, as a freshly cleaved sample presents a surface that is clean and more importantly, smooth at the atomic level. Highly-ordered pyrolytic graphite (HOPG) can produce a similar smoothness to mica with the added advantage that it is inherently hydrophobic, but has the disadvantage that it is not optically clear, and hence of no use in interferometric-based techniques such as the SFA. Thus as noted above, the method of chemical hydrophobisation of mica is widely used in SFA measurements. It is difficult to ascertain the roughness of a chemically adsorbed or bound layer, although it is unlikely to

be *significantly* greater than the mica itself.

When measuring hydrophobic forces between solids in the AFM, the configuration is almost universally a silica or glass sphere glued to the cantilever to act as a probe particle, and a silica or glass flat substrate below. These surfaces are variously hydrophobised by surfactant as with early SFA measurements, or by reaction with organic silanes. The initial silica may have a relatively low surface roughness – on the order of 1 nm root mean squared – but this is significantly rougher than the mica used in the SFA. The effects of the microscopic asperities associated with such roughness are multifarious as noted above, modifying surface forces,[90,91] changing boundary conditions,[23] and modifying the capacity for molecular adsorption,[92] as well as possibly acting as nucleation and pinning sites for surface nanobubbles.[58] As mentioned in the section on bubbles above, purposeful increase of surface roughness by the addition of particles in order to induce superhydrophobicity results in significant amounts of entrained air and very characteristic long-range bridging capillary forces.[61,64]

The manifold and linked effects of roughness make rough surfaces especially challenging for measurement of hydrophobic forces, particularly if the expectation of a short-range force is considered. Particularly in AFM and SFA measurements, the calibration of an accurate separation, central to understanding the range and functional form of any force, is compromised by the roughness of the surface. More troublingly, roughness may change the range and functional form of expected surface forces in complex ways,[90,91,93] further inhibiting quantitative analysis of measured forces. Thus smoother surfaces confer many advantages, explaining the propensity for mica as a substrate in SFA measurements. However, mica's hydrophilicity results in a 'Catch 22' problem that although surfaces are smooth, they require chemical hydrophobisation, with its associated pitfalls. Recently, the dual-path SFA has been developed, finally allowing the use of non-transparent substrates,[94] potentially forming a powerful system for analysis of hydrophobic interactions. An alternative method for achieving extremely smooth surfaces is to employ fluid interfaces (air–water and oil–water) that seek to minimise their area by remaining smooth and featureless.

## Recent progress

We focus here on recent attempts to uncover the nature of the hydrophobic force using novel approaches. For more detail on historical measurements, including those mentioned above, the reader is directed to several thorough reviews on the topic.[9,95]

Kaggwa *et al.* recently measured the interaction between a sharp silicon AFM tip and a silicon wafer in a number of symmetrical and asymmetrical systems using frequency-modulated force spectroscopy (Figure 5a,b).[89] Surfaces were either oxidized using ozone to present a hydrophilic silica surface, or hydrophobised by reaction with hexamethyldisilazane vapour. Two significant features are apparent in the measured force behaviour: firstly, a strong net attraction is seen only for the interaction between a hydrophobic tip and hydrophobic surface (Figure 5b); secondly, for most of the combinations studied, an oscillatory component of the force behaviour is seen, purportedly due to the structuring of water at the surfaces and with a characteristic period of 3 Å (Figure 5a). Several oscillations are seen within the noise limitations of the measurement, although further oscillations of sufficiently low amplitude, as to be masked by experimental noise, may of course be present.

Due to the fact that the AFM tip terminates in such a small radius of curvature ($<$ 1 nm), direct quantification of these forces is challenging, and it is for this reason that a colloidal probe is often used. However, the benefit that the tip confers is comparative insensitivity to surface roughness due to its small lateral dimension, a low level of van der Waals interaction and a high sensitivity to the final few molecular layers of water between the approaching tip and surface. These measurements are clearly complementary to many of the other studies carried out on the hydrophobic force, as they are sensitive to an entirely different length-scale and lateral dimension.

It is important to consider the potential for extraneous effects on such measurements, particularly where dynamic effects such as cantilever oscillation are used. In the measurements of Kaggwa *et al.*, the cantilever is oscillated with a typical amplitude of 2 Å and frequency of 830 kHz.[89] Given that the orientational relaxation time of bulk water is 2.6 ps,[96] potentially rising modestly under confinement,[22,96] we can be confident that the local orientation of water is unaffected on the time-scale of the measurement. Similar experimental setups have been used to probe the viscosity of water under confinement,[21] and so viscous effects would have to be considered in any quantitative analysis. Similarly, the boundary condition at the substrate and tip and the viscoelastic response of liquid around the cantilever could become important, though the structural features of the force curves and the strong evidence for the length-scale of water structure from their qualitative interpretation do not demand such parameters.

At a much larger lateral length scale, our recent work employed fluorocarbon oil droplets of diameter $\approx$100 $\mu$m, refractive index matched to water, to probe the hydrophobic

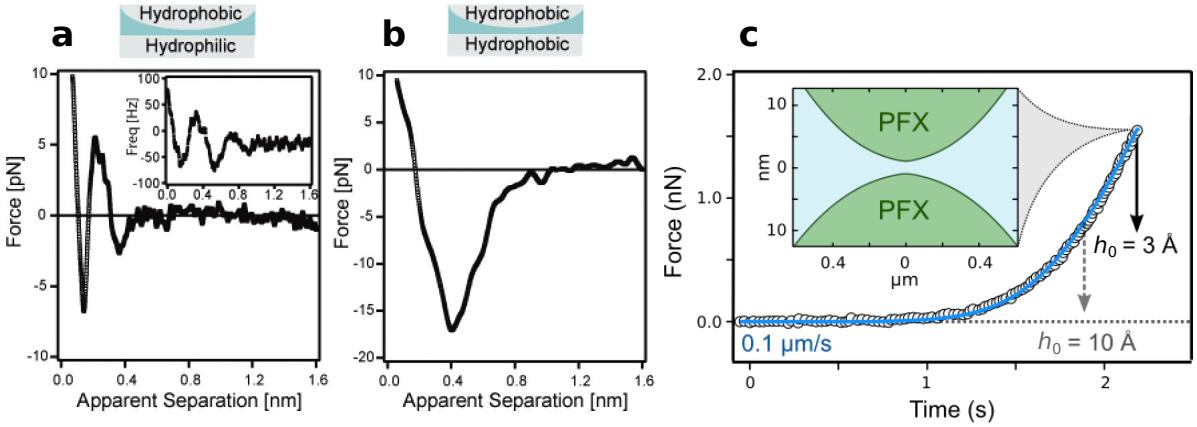


**Fig. 5** Recent advances in measuring the hydrophobic force. a, b) Forces between a hydrophobic AFM tip and a hydrophilic (a), or hydrophobic (b) surface as measured by frequency-modulated AFM. Adapted with permission from Kaggwa *et al.*[89] Copyright 2012, American Chemical Society. c) The force between two oil drops (where PFX is a mixture of perfluorooctane and perfluorobenzene) that are refractive index matched to water, experiencing a moderate electrical double-layer repulsion. The symbols are experimental data from AFM measurement and the inset shows a theoretical prediction of the interface shapes at the moment before coalescence occurs. The black arrow shows the predicted point of coalescence when using an exponential hydrophobic force law with decay length 3 Å, and the dashed arrow shows the predicted coalescence point if the decay length is increased to 10 Å. Drops were pushed together at a pseudo-equilbrium velocity of 100 nm/s. Adapted with permission from Tabor *et al.*[41] Copyright 2013, American Chemical Society.

force.[41] The matched droplets confer a number of unique benefits to the measurement: exceptionally low water solubility, chemical inertness and high intrinsic hydrophobicity, molecularly smooth surfaces, insignificant van der Waals force, no surface modification or charge dissociation effects, no possibility of adsorbed gas or interfacial nanobubbles and 'adaptive' deformable interfaces. However, the disadvantages are clear too: separation between the droplets cannot be measured directly, and the drops are effectively invisible, limiting optical measurements that can be made, and making arrangement of the experiments more challenging than in conventional circumstances; fluorescence and differential interference contrast can be employed to overcome the issues with visualising the droplets. Despite these challenges, interactions between pairs of such droplets were measured in systems where moderate repulsions of different origins such as weak electrical double-layer, van der Waals or hydrodynamic repulsions could be introduced selectively to probe the range and magnitude of the hydrophobic interaction (Figure 5c). It was posited that the aqueous film between the droplets would rupture at the thickness at which the magnitude of the hydrophobic disjoining pressure equalled that due to the repulsion between the droplets.

It was seen that regardless of the type or magnitude of the repulsion between droplets, the aqueous film between them ruptured at a thickness of $\approx 3$ nm. By the careful application of a thoroughly researched and tested physical model[37,97] that accounts for the deformation of the droplets due to surface forces and hydrodynamics, we were able to determine that the attractive hydrophobic disjoining pressure, $\Pi_{HB}$ as a function of separation, $h$ that caused coalescence was best fit by an exponential law, with a decay length, $h_0$ of 3 Å:

$$\Pi_{HB}(h) = -\frac{2\gamma}{h_0}\exp(-h/h_0) \quad (1)$$

The energetic basis for the appearance of the interfacial tension, $\gamma$ is simply that $2\gamma$ is the energy 'surrendered' by the hydrophobic surfaces when they have made contact or coalesced and thus no longer have an interface with water. For oil drops this term is on the order of 100 mN m$^{-1}$ (0.1 J m$^{-2}$), making coalescence highly favourable. The 3 Å decay length that best fits the data aligns with the oscillation period in the work of Kaggwa *et al.* outlined above,[89] and also with the effective separation between water molecules determined theoretically by Lum, Chandler and Weeks.[98] Crudely it is also similar to the effective dimension of water molecules in bulk water, as seen in Figure 1 at the beginning of this article.

Similarly, the effect of boundary conditions and other typically dynamic effects must be considered carefully in the analysis of these measurements, especially when such thin final water films are attained. By carefully comparing results

from pseudo-equilbrium and dynamic experiments, no unexpected effects are revealed, again hinting at the considerable differences.

An additional benefit conferred by the refractive index matching approach to mixing oils is that in systems of dissimilar surfaces, the van der Waals force is still minimised. Thus interactions between a matched oil droplet and any fluid or solid interface could be measured with many of the same advantages.

The concept of measuring forces between dissimilar surfaces has experienced a resurgence recently, and provides additional and valuable information on the role of interactions between water molecules and hydrophobic surfaces. Experiments by Faghihnejad and Zeng explored interactions between mica and polystyrene using the SFA,[99] finding forces that are affected in range and magnitude not only by degassing but also by apparent specific ion effects. A very recent investigation by Li *et al.* of rising bubbles meeting liquid-liquid menisci under the influence of attractive or repulsive van der Waals forces concluded that a short-ranged hydrophobic force was implicated in the film thinning and rupture process.[88] Thus it seems likely that measurements between deformable fluid-fluid and solid-fluid interfaces will complement more traditional solid-solid force measurements as our understanding of the hydrophobic force develops.

## Conclusions and future directions

It seems that each measurement method, due to its inherent strengths and drawbacks has formed a separate piece of the puzzle, uncovering different contributions to unexpected additional attraction between hydrophobic surfaces. Only recently are the pieces forming a cohesive picture of the behaviour of these systems, and permitting a separation of the true hydrophobic force and other interferences that can cause anomalous attractions. It is clear that any 'intrinsic' hydrophobic force due solely to the orientation of water molecules at hydrophobic surfaces is very short range, and there is strong and consistent evidence for a decay length of only 3 Å.[3,15–19,41,89,98]

At larger length-scales, a number of mechanisms appear to operate between hydrophobic solids, producing quite variable forces that are very sensitive to system parameters. The physical rationale for some of these forces has been uncovered – *e.g.*, nanobubbles[76] – but others such as charge rearrangement correlations[71,72] and Hofmeister-type specific ion effects[84] remain unproven, or at least contentious. The fact that degassing liquids when solid surfaces are used decreases the apparent range of the force,[67] although not to the degree that it matches that measured for oil–water interfaces, is further evidence for surface-specific effects.

This serves to highlight the important intrinsic physical differences between the characteristics of liquid–liquid and liquid–gas interfaces as opposed to liquid–solid systems, and may also form the basis for the eventual explanation of surface nanobubbles. The fact that these structures can only exist at solid–water and not oil–water interfaces, despite the high inherent hydrophobicity of the latter, directly implicates the solid nature of the surface in their stability. Due to the much higher solubility of apolar gas molecules in oils than in water, it is simply not possible for them to accumulate at oil–water interfaces in the same way that they are attracted to hydrophobic solids.[69] It could be that their presence, even in very small amounts, results in density changes, disruption to hydrogen bonding or other (as yet unconsidered) effects that are implicated in both measured hydrophobic forces at solid surfaces and surface nanobubbles.

Based on the demonstrable and perplexing differences between measurements between solid interfaces when compared to fluid interfaces, a valuable approach to unravelling such mismatches is to perform experiments using dissimilar surfaces.[88,89,99] The next step may be to revisit the original measurements of Blake and Kitchener[32] but taking advantage of new techniques that can sensitively measure forces in such systems. The ability to perform measurements with oil drops, which may be selected so as to arrange the van der Waals force to be positive, negative or (nearly) absent,[41,88] will undoubtedly provide greater insight. In doing so, contributions from both fluid and solid surfaces can be compared, potentially explaining the different forces seen, and crucially, the mechanistic reason for such differences.

The next major challenge must surely be in the contextualisation of the forces and laws measured to date with respect to molecular systems. The most important manifestation of the hydrophobic force – in the self assembly of the amphiphiles and biomolecules at the heart of life itself – requires an understanding not of extended surfaces, but of molecular systems. Recent work using the nano-scale tip of an AFM cantilever[89] has decreased the effective length-scale of measurement such that this bridge is poised to be crossed, enabling meaningful comparisons to be made. Measuring separations and locations with sufficient precision is becoming more routine, using for example super-resolution fluorescence microscopy,[100] and this will prove crucial to the application of these measurements to soft systems.

In making this molecular connection, the direct measurement of forces must be coupled to – or at least complementary to

– measurements of the orientation and behaviour of the water molecules themselves. Whether this can be achieved spectroscopically using, for example, sum-frequency generation or related techniques, or by reflectivity measurements employing neutrons or X-rays remains to be uncovered.[101] However, it seems that surface-sensitive techniques such as these may provide significant insight into the few molecular layers of water that are surface-adjacent and thus most sensitive to the effects of the hydrophobic surface.

## Acknowledgement

We are grateful to Clayton Radke for valuable discussions on the hydrophobic force and its measurement. This work was supported in part by the Australian Research Council through the provision of Discovery Project funding (DP140100677 and DP110101090).

## References

1 C. Tanford, *The Hydrophobic Effect: Formation of Micelles and Biological Membranes*, John Wiley & Sons, New York, 1973.
2 Y. S. Dijkaev and E. Ruckenstein, *J. Chem. Phys.*, 2009, **130**, 124713/1–10.
3 A. K. Soper, *Chem. Phys.*, 2000, **258**, 121–137.
4 B. Widom, P. Bhimalapuram and K. Koga, *Phys. Chem. Chem. Phys.*, 2003, **5**, 3085–3093.
5 Y.-H. Tsao, S. X. Yang and D. Fennell Evans, *Langmuir*, 1991, **7**, 3154–3159.
6 S. Shimizu and H. S. Chan, *J. Chem. Phys.*, 2000, **113**, 4683–4700.
7 H. K. Christenson and P. M. Claesson, *Adv. Colloid Interface Sci.*, 2001, **91**, 391–436.
8 P. Attard, *Adv. Colloid Interface Sci.*, 2003, **104**, 75–91.
9 E. E. Meyer, J. K. Rosenberg and J. N. Israelachvili, *Proc. Natl. Acad. Sci. U.S.A.*, 2006, **103**, 15739–15746.
10 M. U. Hammer, T. A. Anderson, A. Chaimovich, M. S. Shell and J. N. Israelachvili, *Faraday Discuss.*, 2010, **146**, 299–308.
11 D. Chandler, *Nature*, 2005, **437**, 640–647.
12 C. Tanford, *J. Molec. Biol.*, 1972, **67**, 59–74.
13 C. Tanford, *J. Phys. Chem.*, 1972, **76**, 3020–3024.
14 C. Tanford, *Science*, 1978, **200**, 1012–1018.
15 L. Cheng, P. Fenter, K. L. Nagy, M. L. Schlegel and N. C. Sturchio, *Phys. Rev. Lett.*, 2001, **87**, 156103.
16 M. J. Higgins, M. Polcik, T. Fukuma, J. E. Sader, Y. Nakayama and S. P. Jarvis, *Biophys. J.*, 2006, **91**, 2532–2542.
17 J. H. Hoh, J. P. Cleveland, C. B. Prater, J.-P. Revel and P. K. Hansma, *J. Am. Chem. Soc.*, 1992, **114**, 4918–4920.
18 K. Suzuki, N. Oyabu, K. Kobayashi, K. Matsushige and H. Yamada, *Appl. Phys. Express*, 2011, **4**, 125102.
19 T. Fukuma, K. Kobayashi, K. Matsushige and H. Yamada, *Appl. Phys. Lett.*, 2005, **86**, 193108.
20 T.-D. Li and E. Riedo, *Phy. Rev. Lett.*, 2008, **100**, 106102.
21 D. Ortiz-Young, H.-C. Chiu, S. Kim, K. Voitchovsky and E. Riedo, *Nat. Commun.*, 2013, **4**, 2482.
22 B. Mukherjee, P. K. Maiti, C. Dasgupta and A. K. Sood, *ACS Nano*, 2008, **2**, 1189–1196.
23 O. I. Vinogradova and A. V. Belyaev, *J. Phys.: Condens. Matter*, 2011, **23**, 184104.
24 O. I. Vinogradova, *Langmuir*, 1995, **11**, 2213–2220.
25 T. A. Ho, D. V. Papavassiliou, L. L. Lee and A. Striolo, *Proc. Natl. Acad. Sci. U.S.A.*, 2011, **108**, 16170–16175.
26 B. V. Derjaguin, I. I. Abrikosova and E. M. Lifshitz, *Q. Rev. Chem. Soc.*, 1956, **10**, 295–329.
27 A. Scheludko, *Adv. Colloid Interface Sci.*, 1967, **1**, 391–464.
28 J. C. Froberg, O. J. Rojas and P. M. Claesson, *Int. J. Miner. Process.*, 1999, **56**, 1–30.
29 I. Larson and J. Ralston, in *Encyclopedia of Surface and Colloid Science, Volume 1*, ed. A. T. Hubbard, Marcel Dekker, New York, 2002, ch. Atomic Force Microscopy and Colloid Interaction Forces.
30 L. Wang, D. Sharp, J. Masliyah and Z. Xu, *Langmuir*, 2013, **29**, 3594–3603.
31 D. C. Prieve, *Adv. Colloid Interface Sci.*, 1999, **82**, 93–125.
32 T. D. Blake and J. A. Kitchener, *J. Chem. Soc., Faraday Trans. 1*, 1972, **68**, 1453–1442.
33 R. F. Tabor, F. Grieser, R. R. Dagastine and D. Y. C. Chan, *J. Colloid Interface Sci.*, 2012, **371**, 1–14.
34 R.-H. Yoon and B. S. Aksoy, *J. Colloid Interface Sci.*, 1999, **211**, 1–10.
35 D. Bhatt, J. Newman and C. J. Radke, *J. Phys. Chem. B*, 2003, **107**, 13076–13083.
36 J. N. Israelachvili, Y. Min, M. Akbulut, A. Alig, G. Carver, W. Greene, K. Kristiansen, E. Meyer, N. Pesika, K. Rosenberg and H. Zeng, *Rep. Prog. Phys.*, 2010, **73**, 036601.
37 D. Y. C. Chan, R. Manica and E. Klaseboer, *Soft Matter*, 2011, **7**, 2235–2264.
38 R. F. Tabor, H. Lockie, D. Mair, R. Manica, D. Y. C. Chan, F. Grieser and R. R. Dagastine, *J. Phys. Chem. Lett.*, 2011, **2**, 961–965.
39 V. S. J. Craig, B. W. Ninham and R. M. Pashley, *Langmuir*, 1999, **15**, 1562–1569.
40 R. M. Pashley, P. M. McGuiggan, B. W. Ninham and D. Fennell Evans, *Science*, 1985, **229**, 1088–1089.
41 R. F. Tabor, C. Wu, F. Grieser, R. R. Dagastine and D. Y. C. Chan, *J. Phys. Chem. Lett*, 2013, **4**, 3872–3877.
42 Y. I. Rabinovich and R.-H. Yoon, *Langmuir*, 1994, **10**, 1903–1909.
43 J. N. Israelachvili and R. M. Pashley, *Nature*, 1982, **300**, 341–342.
44 N. Ishida, T. Inoue, M. Miyahara and K. Higashitani, *Langmuir*, 2000, **16**, 6377–6380.
45 X. H. Zhang, A. Quinn and W. A. Ducker, *Langmuir*, 2008, **24**, 4756–4764.
46 J. R. T. Seddon and D. Lohse, *J. Phys.: Condens. Matter*, 2011, **23**, 133001.
47 L. A. Palmer, D. Cookson and R. N. Lamb, *Langmuir*, 2011, **27**, 144–147.
48 C. U. Chan and C.-D. Ohl, *Phys. Rev. Lett.*, 2012, **109**, 174501.
49 S.-T. Lou, Z.-Q. Ouyang, Y. Zhang, X.-J. Li, J. Hua, M.-Q. Li and F.-J. Yang, *J. Vac. Sci. Tech. B*, 2000, **18**, 2573–2575.
50 C.-W. Yang, Y.-H. Lu and I.-S. Hwang, *J. Phys.: Condens. Matter*, 2013, **25**, 184010.
51 J. R. T. Seddon, D. Lohse, W. A. Ducker and V. S. J. Craig, *ChemPhysChem*, 2012, **13**, 2179–2187.
52 W. A. Ducker, *Langmuir*, 2009, **25**, 8907–8910.
53 J. R. T. Seddon, H. J. W. Zandlivet and D. Lohse, *Phys. Rev. Lett.*, 2011, **107**, 116101.
54 R. P. Berkelaar, E. Dietrich, G. A. M. Kip, E. S. Kooij, H. J. W. Zandlivet and D. Lohse, *Soft Matter*, 2014, **10**, 4947–4955.
55 C. E. Brennen, *Cavitation and Bubble Dynamics*, Oxford University Press, Oxford, 1995.
56 F. Caupin and E. Herbert, *C. R. Phys.*, 2006, **7**, 1000–1017.
57 D. Sette and F. Wanderlingh, *Phys. Rev.*, 1962, **125**, 409–417.
58 R. E. Apfel, *J. Acoustic Soc. Am.*, 1970, **48**, 1179–1186.
59 M. A. Hampton, B. C. Donose and A. V. Nguyen, *J. Colloid Interface*

*Sci.*, 2008, **325**, 267–274.
60 X. H. Zhang, A. Kumar and P. J. Scales, *Langmuir*, 2011, **27**, 2484–2491.
61 P. M. Hansson, P. M. Claesson, A. Swerin, W. H. Briscoe, J. Schoelkopf, P. A. G. Gane and E. Thormann, *Phys. Chem. Chem. Phys.*, 2013, **15**, 17893–17902.
62 M. A. Hampton and A. V. Nguyen, *J. Colloid Interface Sci.*, 2009, **333**, 800–806.
63 P. M. Hansson, A. Swerin, J. Schoelkopf, P. A. G. Gane and E. Thormann, *Langmuir*, 2012, **28**, 8026–8034.
64 D. Y. C. Chan, M. H. Uddin, K. L. Cho, I. I. Liaw, R. N. Lamb, G. W. Stevens, F. Grieser and R. R. Dagastine, *Faraday Discuss.*, 2009, **143**, 151–168.
65 E. E. Meyer, Q. Lin, T. Hassenkam, E. Oroudjev and J. N. Israelachvili, *Proc. Natl. Acad. Sci. USA*, 2005, **102**, 6839–6842.
66 J. L. Parker, P. M. Claesson and P. Attard, *J. Phys. Chem.*, 1994, **98**, 8468–8480.
67 N. Ishida, Y. Kusaka and H. Ushijima, *Langmuir*, 2012, **28**, 13952–13959.
68 S. M. Dammer and D. Lohse, *Phys. Rev. Lett.*, 2006, **96**, 206101.
69 C. Sendner, D. Horinek, L. Bocquet and R. R. Netz, *Langmuir*, 2009, **25**, 10768–10781.
70 M. J. Neeson, R. F. Tabor, F. Grieser, R. R. Dagastine and D. Y. C. Chan, *Soft Matter*, 2012, **8**, 11042–11050.
71 R. Podgornik, *J. Chem. Phys.*, 1989, **91**, 5840–5849.
72 S. J. Miklavic, D. Y. C. Chan, L. R. White and T. W. Healy, *J. Phys. Chem.*, 1994, **98**, 9022–9032.
73 S. H. Donaldson, C. T. Lee, B. F. Chmelka and J. N. Israelachvili, *Proc. Natl. Acad. Sci. USA*, 2011, **108**, 15699–15704.
74 N. Ishida, N. Sakamoto, M. Miyahara and K. Higashitani, *Langmuir*, 2000, **16**, 5681–5687.
75 N. N. Gosvami, E. Parsons, C. Marcovich, M. L. Berkowitz, B. W. Hoogenboom and S. Perkin, *RSC Adv.*, 2012, **2**, 4181–4188.
76 N. Ishida, N. Kinoshita, M. Miyahara and K. Higashitani, *J. Colloid Interface Sci.*, 1999, **216**, 387–393.
77 M. Hato, *J. Phys. Chem.*, 1996, **100**, 18530–18538.
78 A. Nakajima, *NPG Asia Materials*, 2011, **3**, 49–56.
79 I. E. Dzaloshinskii, E. M. Lifshitz and L. P. Pitaerskii, *Adv. Phys.*, 1961, **10**, 165–209.
80 J. Mahanty and B. W. Ninham, *Dispersion Forces*, Academic Press, London, 1976.
81 R. R. Dagastine, D. C. Prieve and L. R. White, *J. Colloid Interface Sci.*, 2002, **249**, 78–83.
82 P. J. Scales, F. Grieser and T. W. Healy, *Langmuir*, 1990, **6**, 582–589.
83 R. F. Tabor, C. Wu, H. Lockie, R. Manica, D. Y. C. Chan, F. Grieser and R. R. Dagastine, *Soft Matter*, 2011, **7**, 8977–8983.
84 F. Hofmeister, *Arch. Exp. Pathol. Pharmacol.*, 1888, **24**, 247–260.
85 Y. Koga and P. Westh, *Phys. Chem. Chem. Phys.*, 2014, **16**, 335–344.
86 T. Lopez-Leon, J. M. Lopez-Lopez, G. Odriozola, D. Bastos-Gonzalez and J. L. Ortega-Vinuesa, *Soft Matter*, 2010, **6**, 1114–1116.
87 D. F. Parsons, M. Bostrom, T. J. Maceina, A. Salis and B. W. Ninham, *Langmuir*, 2010, **26**, 3323–3328.
88 E. Q. Li, I. U. Vakarelski, D. Y. C. Chan and S. T. Thoroddsen, *Langmuir*, 2014, **30**, 5162–5169.
89 G. B. Kaggwa, P. C. Nalam, J. I. Kilpatrick, N. D. Spencer and S. P. Jarvis, *Langmuir*, 2012, **28**, 6589–6594.
90 N. Sun and J. Y. Walz, *J. Colloid Interface Sci.*, 2001, **234**, 90–105.
91 R. R. Dagastine, M. Bevan, L. R. White and D. C. Prieve, *J. Adhes.*, 2004, **80**, 365–394.
92 S. Wu, L. Shi, L. B. Garfield, R. F. Tabor, A. Striolo and B. P. Grady, *Langmuir*, 2011, **27**, 6091–6098.
93 M. Valtiner, X. Banquy, K. Kristiansen, G. W. Greene and J. N. Israelachvili, *Langmuir*, 2012, **28**, 13080–13093.
94 H. Kawai, H. Sakuma, M. Mizukami, T. Abe, Y. Fukao, H. Tajima and K. Kurihara, *Rev. Sci. Instrum.*, 2008, **79**, 043701.
95 H. K. Christenson, J. F. Fang and B. W. Ninham, *J. Phys. Chem.*, 1990, **94**, 8004–8006.
96 D. B. Fenn, E. E. abd Wong and M. D. Fayer, *Proc. Natl. Acad. Sci. U.S.A.*, 2009, **106**, 15243–15248.
97 D. Y. C. Chan, E. Klaseboer and R. Manica, *Adv. Colloid Interface Sci.*, 2011, **165**, 70–90.
98 K. Lum, D. Chandler and J. D. Weeks, *J. Phys. Chem. B*, 1999, **103**, 4570–4577.
99 A. Faghihnejad and H. Zeng, *Langmuir*, 2013, **29**, 12443–12451.
100 D. R. Whelan, T. Holm, M. Sauer and T. D. M. Bell, *Aus. J. Chem.*, 2013, **67**, 179–183.
101 M. Lucas and E. Riedo, *Rev. Sci. Instrum.*, 2012, **83**, 061101.